American Mineralogist, Volume 71, pages 1285–1296, 1986

Alkali feldspars: Structural state determined from composition and optic axial angle $2V$

Shu-Chun Su,[1] Paul H. Ribbe, F. Donald Bloss

Department of Geological Sciences, Virginia Polytechnic Institute and State University, Blacksburg, Virginia 24061, U.S.A.

Abstract

For the *entire* homogeneous alkali feldspar series, the Al content (Σt_1) of the T_1 tetrahedral sites is a measure of structural state: $\Sigma t_1 \equiv 2t_1$ for monoclinic and $\Sigma t_1 \equiv (t_1o + t_1m)$ for triclinic specimens. Σt_1 can be conveniently estimated from V_X (one-half of the optic axial angle $2V_X$) and X_{Or} (mole fraction of $KAlSi_3O_8$) by using a simple determinative diagram or the equation

$$\Sigma t_1 = \frac{b_0 + b_1X_{Or} + b_2X_{Or}\sin^2V_X + b_3\sin^2V_X}{a_0 + a_1X_{Or} + a_2X_{Or}\sin^2V_X + a_3\sin^2V_X}.$$

Three sets of coefficients (multiplied by 1000 in the following table) account for three regions of $2V_X$-X_{Or} space: case A, $X_{Or} \leq 0.6$; case B, $X_{Or} > 0.6$ and O.A.P. (optic axial plane) perpendicular or approximately perpendicular to (010); and case C, $X_{Or} > 0.6$ and O.A.P. parallel to (010).

Case	a_0	a_1	a_2	a_3	b_0	b_1	b_2	b_3
A	4.08	−2.35	0.95	−1.28	1.52	−0.18	−1.74	2.88
B	1.69	1.63	−2.33	0.69	0.11	2.17	−2.70	3.46
C	−1.69	−1.63	−0.70	2.38	−0.11	−2.17	−0.53	3.57

Tested using data for 109 alkali feldspars whose Σt_1 values were independently estimated from lattice parameters and/or mean T–O bond lengths from crystal-structure analyses, this model estimates Σt_1 within ±0.02 for 83% and ±0.04 for 97% of them. This precision is the same as that from various models that rely on lattice parameters for estimation of Σt_1, e.g., *b-c*, *b-c**, $2\theta(060)$-$2\theta(\bar{2}04)$ methods, etc.

The model was developed by assuming that the principal refractive indices—symbolized as n_a, n_b, and n_c and defined as the principal refractive indices for light vibrating parallel or nearly parallel to crystallographic axes **a, b,** and **c,** respectively—vary linearly with Σt_1 for the high sanidine–low microcline series and for the low albite–high albite (or analbite) series. However, for the high albite–high sanidine solid-solution series, as well as the low albite–low microcline series, neither density nor principal refractive indices vary linearly across the entire composition range, but they closely approached linearity in segments between $0.0 \leq X_{Or} < 0.6$ and $0.6 < X_{Or} \leq 1.0$.

Introduction

Quantitative measures of the structural state of alkali feldspars have been employed in geologic investigations for many years. Kroll and Ribbe (1983, p. 95) listed 30 studies in the period 1975 to 1982 that involved use of unit-cell parameters for that purpose. Wright and Stewart (1968) introduced the now familiar *b-c* plot, which was quantified by Stewart and Ribbe (1969) in terms of $\Sigma t_1 = 2t_1$ or $(t_1o + t_1m)$, depending on whether the feldspar is monoclinic $C2/m$ or triclinic $C\bar{1}$. [The symbols t_1, t_1o, and t_1m indicate the fractional Al content of the T_1, T_1O, and T_1m tetrahedral sites in the structure of the alkali feldspar.] Kroll and Ribbe (in prep.) have summarized the more recent equations for determining structural state from lattice parameters. However, separating feldspar from rocks and indexing X-ray powder-diffraction patterns for least-squares refinement of unit-cell parameters is tedious at best. Short cuts involving *d*-spacings of a certain few peaks in a powder pattern were introduced by Hewlett (1959), refined by Wright (1968), and have been put in equation form by Kroll and Ribbe (in prep.). All the while and for decades preceding the development of X-ray methods, use of optic axial angle $2V$ as a quantitative measure of structural state (where composition is known) has tantalized petrologists. Stewart (1974) concluded that $2V$ depended "on the Al content of the T_1 sites" (Σt_1) in isocompositional series, and Su et al. (1984) confirmed this quantitatively for the K-rich low microcline–high sanidine series. The very careful work of Bertelmann et al. (1985)

[1] Permanent address: Institute of Geology, Chinese Academy of Sciences, Beijing, the People's Republic of China.

0003–004X/86/1112–1285$02.00

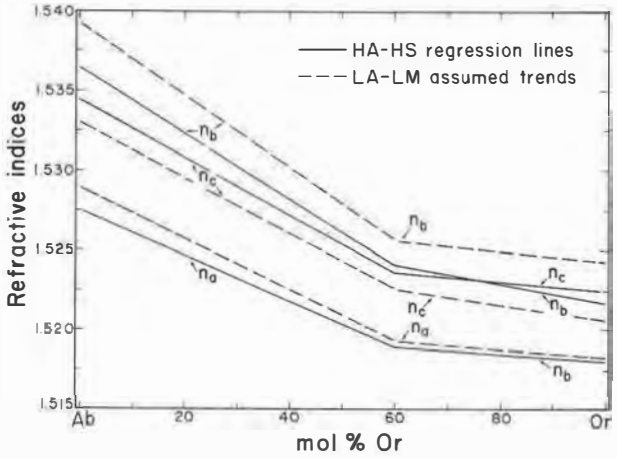

Fig. 1. Variation trends of refractive indices of alkali feldspars vs. mole percent Or. Solid lines are the observed trends for HA–HS series with $\Sigma t_1 = 0.60$ from Su et al. (1986b). Dashed lines are the assumed trends for LA–LM series with $\Sigma t_1 = 1.00$.

demonstrated the interdependence of composition, Σt_1, and $2V_X$ for a limited range of monoclinic K-rich feldspars, $0.69 \leq X_{Or} \leq 0.82$.

This paper attempts to relate quantitatively the relationships among compositions (Or), structural states (Σt_1) and optic axial angles ($2V$) for the *entire* range of homogeneous alkali feldspars. In order to do this, the optical properties of the limiting series around the periphery of the quadrilateral on a *b-c* plot—i.e., low albite–low microcline (LA–LM) series, high albite (analbite)–high sanidine [HA (AA)–HS] series, LA–HA (AA) series, and LM–HS series—were first established.

Optical properties of the limiting series of alkali feldspars

The assumption that refractive indices vary linearly with $\Sigma t_1 = 2t_1$ or $(t_1o + t_1m)$ in the LM–HS series was substantiated by Su et al. (1984). Fortunately, for purposes of comparison with this order-disorder series, the refractive indices of the LA–HA series were also found to vary linearly with Σt_1 (Su et al., 1985, 1986a). Preliminary optical and X-ray investigation of the highly disordered high albite–high sanidine (HA–HS) solid-solution series (Warner et al., 1984) led to somewhat misleading conclusions that since have been superseded by studies described by Su et al. (1986b).

In all three of these studies, n_a, n_b, and n_c were defined as the principal refractive indices for light vibrating parallel or nearly parallel to the **a, b,** and **c** crystallographic axes, respectively (Su et al., 1984; Bloss, 1985). Accordingly, $n_a = n_\alpha$ for all alkali feldspars; $n_b = n_\beta$ and $n_c = n_\gamma$ for those high-temperature, monoclinic, K-rich sanidines whose optic axial planes (O.A.P.) are parallel to (010); and $n_b = n_\gamma$ and $n_c = n_\beta$ for all the triclinic and some of the monoclinic alkali feldspars whose optic axial planes are perpendicular or approximately perpendicular to (010). Use of the symbols n_a, n_b, and n_c for the principal refractive indices obviates the confusion that has long surrounded the variation of optical properties of different series in the system $NaAlSi_3O_8$-$KAlSi_3O_8$. It has been particularly useful in delineating the variation of the optic axial angle $2V$, which must vary sigmoidally with Σt_1 if the refractive indices vary linearly with Σt_1 within an isocompositional order-disorder series or if they vary linearly with mole percent Or within an alkali-exchange or a solid-solution series of feldspars that have a particular structural state.

The LA–LM solid-solution series has eluded detailed optical investigation because no natural single crystals exist except for nearly pure endmembers. However, $2V$ has been measured on a few minute grains of alkali-exchanged specimens whose lattice parameters were determined by X-ray powder diffractometry (Rankin, 1967, on specimens of Orville, 1967). The assumptions involved in arriving at a variation trend for the refractive indices of this series relative to Or content will be discussed later.

Variation of $2V$ with composition and structural state

The optic angle $2V$ is of particular interest for the alkali feldspars. Minor substitutions of [(Ca,Ba,Sr) + Al] for [(Na,K) + Si] and Fe^{3+} for Al all tend to increase the refractive indices (Hewlett, 1959; Plas, 1966; Smith, 1974), but effects on birefringences (and thus $2V$) are relatively small. Although some scatter possibly due to these effects was unaccounted for, Stewart (1974, updated by Stewart and Ribbe, 1983) found that a plot of the *b* and *c* unit-cell parameters for more than 80 alkali feldspars whose $2V$ values were known could be contoured with straight lines for $2V$ rather well. Because the *b-c* plot has long been established as a quantitative indicator of structural state (Σt_1) for the entire range of alkali feldspars (Stewart and Ribbe, 1969), it is obvious that there exists some *quantitative* relationship among $2V$, Σt_1, and Or. This was implied by Tuttle (1952) and again by Hewlett (1959), both of whom used optical data from Spencer (1937) as well as their own.

Smith (1974, Fig. 8-5, p. 380) plotted $2V$ as a function of mole percent Or for synthetic and for perthitic, nonperthitic, and heated natural alkali feldspars. In so doing, he traced the approximate location of the solvus and roughly indicated (with straight lines) the limiting HA–HS and LA–LM series, as did Bambauer et al. (1979, Fig. 223–232, p. 123). Smith's Figure 8-6 (p. 383) summarizes the $2V$ versus mole percent Or data of Wright and Stewart (1968) and Rankin (1967) for natural and ion-exchanged alkali feldspars. Smith asked, "Is it possible to go further and make a quantitative structural interpretation of the $2V$,Or diagram? Unquestionably, there is a strong tendency for the vertical position on the diagram to correlate with Si,Al order-disorder, but it seems the correlation is somewhat imperfect." Certainly part of the imperfection may have resulted from compositional impurities and from poorly characterized specimens [for example, wide ranges of $2V$ on grains from an alkali-exchanged powder must indicate that either bulk composition and/or structural state differ from grain to grain (cf. Rankin, 1967)]. Sub-

microscopic twinning, exsolution, and strain will also affect $2V$. But much of the imperfection must be attributed to the model that has been used until now. The effects of (Al,Si) ordering and composition on $2V$ in homogeneous feldspar can be properly interpreted only in terms of their effects on refractive indices, which, in turn, determine the magnitude and sign of $2V$ as well as the orientation of the optic axial plane. Based on this approach, we have developed a quantitative model for this system.

Assumptions for a model relating $2V$ to structural state and composition

As documented by Su et al. (1984) and Su et al. (1986b) and discussed above, our model for the variation of $2V$ with structural state at constant composition in alkali feldspars assumes that (1) n_a, n_b, and n_c vary linearly with total Al (Σt_1) in the two T_1 tetrahedral sites of monoclinic and in the T_1O and T_1m sites of triclinic feldspars in (a) the LA–HA series and (b) the LM–HS series and (2) by extension of assumption 1, n_a, n_b, and n_c vary linearly with Σt_1 for *all* isocompositional series of alkali feldspars, without regard to the symmetry of individual members.

Furthermore, as documented by Su et al. (1986b), our model for the variation of $2V$ with composition for a series of alkali feldspars with high structural states, $0.50 \leq \Sigma t_1 \leq 0.65$ (mean $\Sigma t_1 = 0.60$), assumes that (3) n_a, n_b, and n_c each vary in two linear segments with mole percent Or for the HA (AA)–HS series, reflecting the variation in density with mole percent Or of the same series (see Fig. 2, Su et al., 1986b). The first linear segment has a relatively steep negative slope between Or_0 and Or_{60}, and the second is much flatter between Or_{60} and Or_{100} (Fig. 1).

Finally, the variation of $2V$ with mole percent Or for the LA–LM solid-solution series ($\Sigma t_1 = 1.0$) assumes that (4) n_a, n_b, and n_c vary with mole percent Or in the same manner as for the HA–HS series and mimic the variation in density for the LA–LM alkali-exchange series. The assumed trends of the two-segment model (Fig. 1) are discussed below.

Among the above, only assumption 4 is not directly supported by refractive-index data. This is because data are nonexistent, except for the endmembers. The two-segment model in Figure 1 is based by analogy on the variation of the indices with composition in the HA–HS series. The Gladstone-Dale relationship and the density curve for the LA–LM series (Su et al., 1986b, Fig. 2) give us reason to expect that the analogy is valid and that the Or_{60} point is at or near the point at which the slopes of the linear segments change.

Additional support is found in the fact that the highest $2V_X$ value measured by Rankin (1967) in each sample of the alkali-exchanged feldspars of Orville (1967) plots very nearly on the $2V_X$ versus mole percent Or curve calculated from assumption 4 for Σt_1 (see the solid triangle symbols in Fig. 2). This would not be true, for example, if one assumed straight-line variations in n_a, n_b, and n_c with mole percent Or between LA and LM. Furthermore, small adjustments to the slopes of the segments or even the point of flexure would not change partial birefringences substantially and thus would affect the calculated $2V_X$ curve only very slightly. Bambauer et al. (1979, Fig. 228–232, p. 123) obtained a $2V$ curve similar to ours, but gave no justification for it.

Selection of $2V$ and refractive indices of endmembers

If assumptions 1 to 4 are valid, then the immediate problem is to choose refractive indices and $2V$ for the LA, HA (AA), HS, and LM endmembers and the Or_{60} flexure point (Table 1) that will permit calculation of a working diagram of $2V$ versus mole percent Or contoured for Σt_1 (Fig. 2). Of course, this determinative diagram must reproduce Σt_1 values calculated by lattice-parameter methods on the same specimens. Our requirement is that the standard error of estimate for Figure 2 be about the same as that for determining Σt_1 from lattice parameters, i.e., 0.02 (Kroll and Ribbe, 1983).

Three additional constraints were also observed.

Constraint (a). The optic axial angles calculated from these hypothetical refractive indices must be in agreement with $2V_X$ values of 103° for LA and 45° for HA (AA) [both pure $NaAlSi_3O_8$ with $\Sigma t_1 = 1.0$ and 0.5, respectively] and 82.2° for LM and 64° for HS [both pure $KAlSi_3O_8$ with $\Sigma t_1 = 1.0$ and 0.5, respectively].

Relative to constraint (a), the choice of 103° for LA is based on the following data: 103° (Ramona, California; Smith, 1958), 103.4° (Clear Creek, California; Su et al., 1986a), 103° and 102.9° (Amelia, Virginia; Tuttle, 1952; Wolfe, 1976), 103° and 102.5° (Tiburon, California; Crawford, 1966; Su, 1986). Burri et al. (1967) and Marfunin (1966) also chose 103° for LA.

Our choice of 45° as $2V_X$ for HA took into consideration the following previous measurements: (1) 45°–55° for heated albites and ~45° for synthetic albites (Tuttle and Bowen, 1958); (2) 64° and 40° on heated Amelia albites (Laves and Chaisson, 1950); (3) 50° on heated vein albite (Schneider, 1957); (4) 45° on heated Amelia albite and 47° on heated Ramona albite (Smith, 1958); (5) 47° by extrapolation of Raase and Kern's (1969, Fig. 2, p. 229) data to completely disordered albite. Burri et al. (1967) and Bambauer et al. (1979) chose 50° for their hypothetical endmember high albites, but on the basis of the above evidence, 45° is probably a better value. In fact, our choice of 45° for HA is based both on this and on the extrapolated $2V_X$ of 44.8° determined for the series of heated Clear Creek albites using Equation 8 in Su et al. (1986a).

A value of $2V_X = 82.2°$ was chosen for LM in part because it is near the $2V_X$ of 82.5° observed in the structurally analyzed, fully ordered low microcline, from Pellotsalo, Lake Lagoda, USSR (Table 1, $\Sigma t_1 = 1.0$, Or_{95}; Brown and Bailey, 1964; cf. a new crystal-structure refinement by Blasi et al., 1985). Furthermore, when testing the $2V_X$-Σt_1-Or model, use of 83° and 84° for hypothetical LM consistently underestimated Σt_1 for the more-ordered K-rich feldspars, whereas use of values lower than 82° had the opposite effect.

The choice of 64° as the $2V_X$ value for the HS endmember was based in part on the $2V_X = 63°$, O.A.P. = (010), for a synthetic K-feldspar measured by Tuttle (1952, p. 557) and on an extrapolated $2V_X = 63°$ at Or_{100} for 23 heated alkali feldspars studied by Spencer (1937; also see Tuttle, 1952, Fig. 1). Tuttle (1952) did not publish any X-ray data for his synthetic K-feldspar, so it is not known whether it is completely disordered ($\Sigma t_1 = 0.5$).

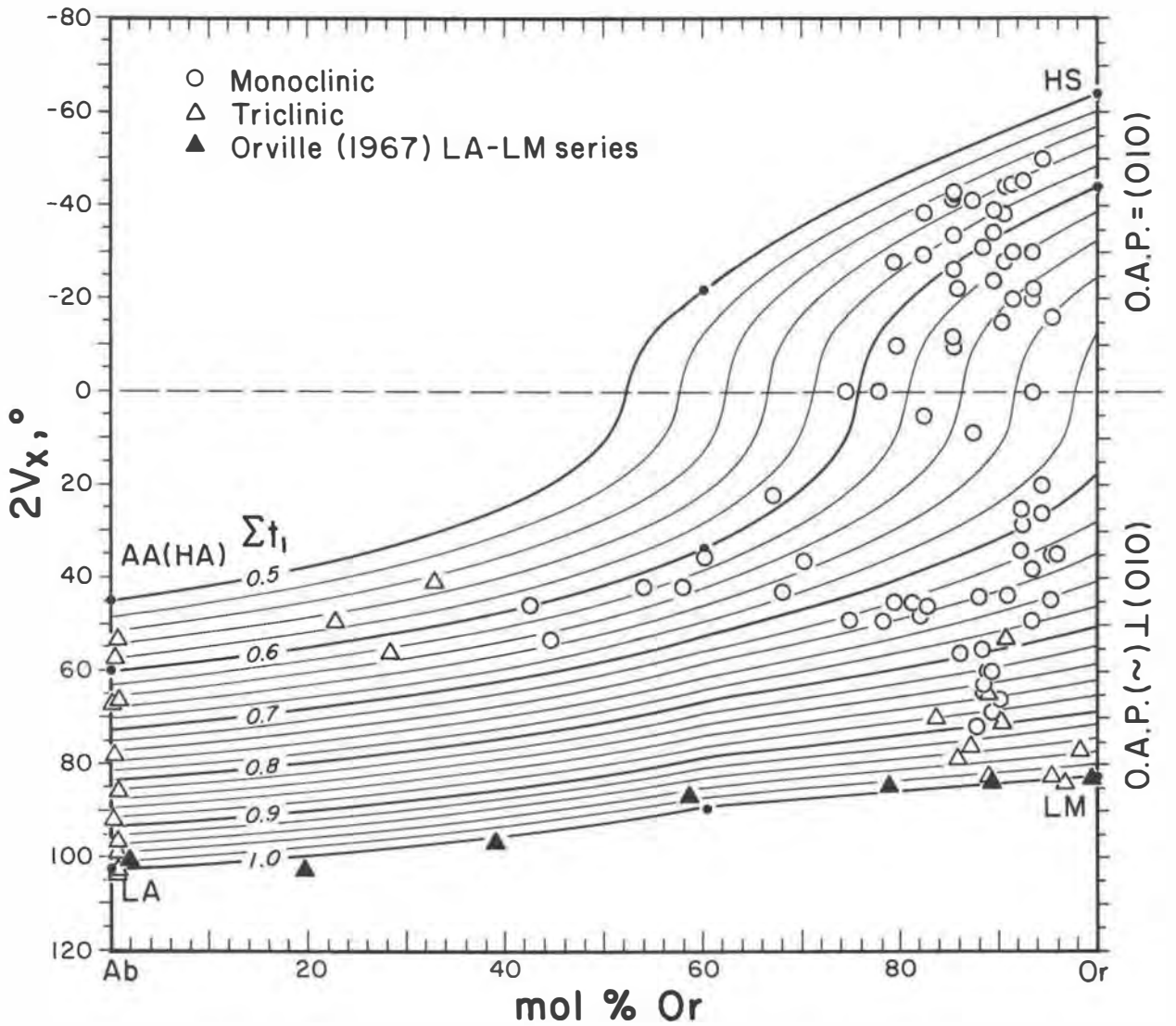

Fig. 2. Plot of $2V_X$ versus mole percent Or contoured for Σt_1: AA = analbite, i.e., a disordered albite with $t_1o = t_1m$ and $t_2o = t_2m$, which will invert to monoclinic symmetry at temperatures above 980°C; other symbols as elsewhere in text. The 109 data from Table 1 are plotted here. Solid triangles represent the largest $2V_X$ value measured by Rankin (1967) on each of the compositions in the LA–LM alkali-exchange series of Orville (1967).

Spencer (1937) mentioned that some of the feldspars he heated had not reached equilibrium. Therefore, the 63° value might not represent a completely disordered HS endmember. Ultimately, the choice of 64° was made in the process of testing our $2V_X$-Σt_1-Or model (as discussed below). It was found that if 63° is chosen, the model tends to underestimate slightly the Σt_1 of sanidines with O.A.P. = (010), i.e., the Σt_1 values read from an early version of Figure 2 were usually lower than Σt_1 calculated from lattice parameters. However, if 64° is chosen, a noticeably (though only slightly) better fit resulted for sanidines.

Constraint (b). Hypothetical n_a, n_b, and n_c values chosen for each endmember must exactly reproduce the $2V_X$ values in constraint (a) and agree with observed or extrapolated refractive indices accepted for HA (AA), LA, LS, and LM to within the standard error of routine measurements.

Discussion of constraint (b) is complicated by the fact that the 32 specimens in the HA–HS series investigated by Su et al. (1986b) have an average structural state of $\Sigma t_1 = 0.60$ rather than 0.50 for the (hypothetically) completely disordered series. The indices for the endmembers of the $\Sigma t_1 = 0.60$ series are predicted from the regression equations given in Table 3 of Su et al. (1986b), but the hypothetical values used in constructing Figure 2 (see Table 1) had to be slightly adjusted from the predicted indices. Adjustments to the indices amount to ±0.0003 or less and are well within the standard errors of estimates of the regression equations and also within twice the standard error ($2\sigma = 0.0006$) for careful refractive-index measurement using conventional double-variation methods.

For the LA–LM series, data are only available for the LA and LM endmembers. The refractive indices and the calculated $2V_X$ values chosen for the hypothetical LA are very close to the arithmetic means obtained for the four natural low albites listed as

Table 1. Optical data of some natural and heated alkali feldspars and extrapolated values for endmembers from other sources

Σt_1	Or (mol%)	An (mol%)	Description	n_a	n_c	n_b	$2V_x$ (°)	Ref
1.00	0.3	0.0	Low albite Clear Creak, California	1.5288(1)	1.5329(2)	1.5394(2)	103.4	5
0.99	0.5	0.2	Low albite Tiburon, California	1.5290(2)	1.5331(2)	1.5395(1)	102.5	7, 8
1.00	0.8	1.2	Low albite Amelia, Virginia	1.5290(2)	1.5330(2)	1.5388(2)	102.9	3, 9
	1.1	0.2	Low albite Ramona, California	1.5286(3)	1.5326(3)	1.5388(3)	103.0	4
1.00	0.0	0.0	Low albite Hypothetical	1.5289	1.5329	1.5393	103.0	
1.00	60.0	0.0	Na microcline Hypothetical	1.5194	1.5226	1.5257	89.2	
1.00	95.0	0.0	Low microcline Pellatsalo, USSR	1.5178(?)	1.5217(?)	1.5247(?)	82.5	1
0.99	98.0	0.0	Low microcline Pontiskalk, Switzerland	1.5178(?)	1.5218(?)	1.5243(?)	77.0	2
1.00	100.0	0.0	Low microcline Hypothetical	1.5183	1.5217	1.5243	82.2	
0.60	0.0	0.0	High albite Extrapolated	1.5276(8)	1.5345(6)	1.5264(8)		4
0.60	0.0	0.0	High albite (analbite) Hypothetical	1.5276	1.5344	1.5267	60.3	
0.60	60.0	0.0	Na high sanidine Extrapolated	1.5188(8)	1.5238(8)	1.5242(9)		6
0.60	60.0	0.0	Na high sanidine Hypothetical	1.5186	1.5238	1.5243	33.4	
0.60	100.0	0.0	High sanidine Extrapolated	1.5179(8)	1.5225(8)	1.5217(9)		6
0.60	100.0	0.0	High sanidine Hypothetical	1.5176	1.5227	1.5220	−44.1	
0.50	0.0	0.0	High albite Hypothetical	1.5273	1.5348	1.5361	45.0	
0.50	60.0	0.0	Na high sanidine Hypothetical	1.5185	1.5242	1.5240	−21.4	
0.50	100.0	0.0	High sanidine Hypothetical	1.5174	1.5229	1.5214	−64.0	

Note: These data are used as reference values in selecting refractive indices and optic angles of "hypothetical" endmembers or Or_{60} members. The values for the "hypothetical" reference points are the ones used to construct Figure 2. References are as follows: (1) Bailey, 1969. (2) Finney and Bailey, 1964. (3) Harlow and Brown, 1980. (4) Smith, 1958. (5) Su et al., 1986a. (6) Su et al., 1986b. (7) Su, 1986. (8) Wainwright and Starkey, 1968. (9) Wolfe, 1976.

reference values in Table 1. Only two sets of refractive indices were available for LM, one from the aforementioned Pellatsalo microcline and the other from the Pontiskalk formation, Switzerland (Σt_1 = 0.99, Or_{98}, Finney and Bailey, 1964). Since the composition of Pontiskalk microcline is closer to Or_{100}, its n_b and n_c values were assigned to hypothetical LM. However, in order to obtain a calculated $2V_X$ of 82.2°, a hypothetical n_a value had to be chosen that is 0.0005 higher than that of the Pontiskalk microcline.

The index values for hypothetical HA and HS at $\Sigma t_1 = 0.50$ were obtained by linear extrapolation from LA and LM through the HA and HS points at $\Sigma t_1 = 0.60$ (assumptions 1 and 2) to reproduce $2V_X$ values of 45° and 64°. See Table 1.

Constraint (c). Hypothetical n_a, n_b, and n_c values for the flexures at Or_{60} must agree within the related standard errors of estimates with those predicted by the regression equations in Table 3 of Su et al. (1986b) for the $\Sigma t_1 = 0.60$ series.

Constraint (c) was easily accommodated by the values listed in Table 1. However, the corresponding values for Or_{60} in the $\Sigma t_1 = 1.0$ series (Table 1) were chosen rather subjectively from the LA–LM curves in Figure 1. Their values were confirmed by the fact that $2V_X = 89°$ agrees reasonably well with Rankin's (1967) value of 86° for Or_{58}. The reference n_a, n_b, and n_c indices for Or_{60} at $\Sigma t_1 = 0.5$ were obtained by linear extrapolation of their respective values at $\Sigma t_1 = 1.0$ and 0.6, based on assumptions 1 and 2 (see App. 1 for detailed mathematical treatments).

Construction of the determinative diagram

A $2V_X$ versus Or diagram (Fig. 2) was contoured for Σt_1 using the refractive indices for the hypothetical LA, HA (AA), HS, and LM endmembers and Or_{60} of low and high

Table 2. Coefficients of Equation 1 for calculating Σt_1 from X_{Or} and $2V_X$

Coefficient	Case A	Case B	Case C
a_0	0.00408	0.001 69	−0.001 69
a_1	−0.002 35	0.001 63	−0.001 63
a_2	0.000 95	−0.002 33	−0.000 70
a_3	−0.001 28	0.000 69	0.002 38
b_0	0.001 52	0.000 11	−0.000 11
b_1	−0.000 18	0.002 17	−0.002 17
b_2	−0.001 74	−0.002 70	−0.000 53
b_3	0.002 88	0.003 46	0.003 57

Note: Case A, $X_{Or} \leq 0.6$, case B, $X_{Or} > 0.6$ and O.A.P. (~) $\perp$ (010), and case C, $X_{Or} > 0.6$ and O.A.P. = (010). For derivation, see Appendix 1.

Table 3. Alkali feldspars, their compositions, $2V_x$ values, and direct and reciprocal cell edges b and c^*, and Al content of the T_1 tetrahedral sites, Σt_1

No.	Sample	Or (mol%)	Non-alkali	Sym	$2V_x$ (°)	b (Å)	c^* (Å^{-1})	Σt_1 (b, c^*)	Σt_1 ($2V$, Or)	Δ	Ref
1	5A1	94.0	2.0	M	−50.0	13.032	0.15503	0.55	0.55	0	14
2	1B1	92.0	2.0	M	−45.0	13.031	0.15498	0.57	0.56	0.01	14
3	SAN-SP-C	90.8	1.1	M	−44.5	13.030	0.15506	0.55	0.56	−0.01	3
4	S1A33-4	90.0	1.0	M	−44.0	13.032	0.15498	0.56	0.56	0	27
5	7002H	85.0	0.5	M	−42.6	13.033	0.15510	0.54	0.54	0	13, 24
6	SAGT-N	85.0	1.0	M	−42.0	13.033	0.15501	0.55	0.55	0	9
7	SANN-R	85.0	1.0	M	−42.0	13.033	0.15501	0.55	0.55	0	9
8	SANI-R	85.0	1.0	M	−41.5	13.033	0.15501	0.55	0.55	0	9
9	SVG3-N	85.0	1.0	M	−41.5	13.033	0.15501	0.55	0.55	0	9
10	SV-17T	87.0	2.0	M	−41.0	13.037	0.15496	0.55	0.56	−0.01	25
11	S1A33-3	89.0	1.0	M	−39.0	13.032	0.15498	0.56	0.58	−0.02	27
12	SV-1050	82.0	2.0	M	−38.4	13.034	0.15502	0.54	0.55	−0.01	12
13	S1A43-4	90.0	1.0	M	−38.0	13.026	0.15491	0.59	0.58	0.01	27
14	S1A44-2	89.0	1.0	M	−34.0	13.023	0.15494	0.60	0.59	0.01	27
15	SAND-R	85.0	1.0	M	−33.8	13.026	0.15494	0.59	0.58	0.01	9
16	SANG-N	85.0	1.0	M	−33.8	13.026	0.15494	0.59	0.58	0.01	9
17	SAAT-R	85.0	1.0	M	−33.6	13.026	0.15494	0.59	0.58	0.01	9
18	S1A43-3	88.0	1.0	M	−31.0	13.019	0.15496	0.61	0.60	0.01	27
19	S1A33-2	91.0	1.0	M	−30.0	13.025	0.15490	0.60	0.61	−0.01	27
20	2A4	93.0	2.0	M	−30.0	13.017	0.15488	0.63	0.62	0.01	14
21	SV-850	82.0	2.0	M	−29.5	13.026	0.15498	0.58	0.58	0	12
22	HEW-11	79.0	5.3	M	−28.0	13.015	0.15500	0.61	0.57	0.04	6, 11
23	S1A43-2	90.0	1.0	M	−28.0	13.025	0.15491	0.60	0.62	−0.02	27
24	SATO-R	85.0	1.0	M	−26.3	13.026	0.15492	0.59	0.60	−0.01	9
25	S1A44-1	89.0	1.0	M	−24.0	13.021	0.15487	0.62	0.62	0	27
26	7002	85.4	1.0	M	−22.0	13.015	0.15497	0.62	0.61	0.01	13
27	2B4-2	93.0	2.0	M	−22.0	13.018	0.15480	0.64	0.64	0	14
28	S1A33-1	91.0	1.0	M	−20.0	13.024	0.15483	0.61	0.64	−0.03	27
29	2B4-1	93.0	2.0	M	−20.0	13.017	0.15489	0.63	0.65	−0.02	14
30	2B15-2	95.0	2.0	M	−16.0	13.014	0.15473	0.66	0.66	0	14
31	S1A43-1	90.0	1.0	M	−15.0	13.020	0.15484	0.63	0.64	−0.01	27
32	SAGA-R	85.0	1.0	M	−11.8	13.019	0.15488	0.62	0.63	−0.01	9
33	SANU-N	85.0	1.0	M	−11.8	13.019	0.15488	0.62	0.63	−0.01	9
34	SVG1-N	85.0	1.0	M	−11.8	13.019	0.15488	0.62	0.63	−0.01	9
35	HEW-12	79.2	3.0	M	−10.0	13.018	0.15515	0.57	0.61	−0.04	6, 11
36	STOT-R	85.0	1.0	M	−9.0	13.019	0.15488	0.62	0.63	−0.01	9
37	HEW-2	74.0	1.0	M	0.0	13.010	0.15511	0.60	0.59	0.01	6, 11
38	HEW-1	77.4	2.9	M	0.0	13.017	0.15508	0.59	0.61	−0.02	6, 11
39	2B15-1	93.0	2.0	M	0.0	13.011	0.15478	0.66	0.66	0	14
40	SV-0	82.0	2.0	M	5.2	13.023	0.15486	0.61	0.63	−0.02	12
41	SV-17	87.0	2.0	M	9.0	13.028	0.15481	0.61	0.65	−0.04	25
42	2B-6	94.0	2.0	M	20.0	13.008	0.15471	0.69	0.69	0	14
43	HEW-13	66.7	1.7	M	22.0	13.010	0.15506	0.61	0.59	0.02	6, 11
44	2B11-2	92.0	2.0	M	25.0	13.003	0.15473	0.70	0.69	0.01	14
45	2B12	94.0	2.0	M	26.0	13.005	0.15466	0.71	0.70	0.01	14
46	2B131	92.0	2.0	M	28.0	13.004	0.15469	0.70	0.70	0	14
47	2B31	92.0	2.0	M	34.0	12.997	0.15462	0.74	0.71	0.03	14
48	SP-A	95.4	2.0	M	34.8	12.989	0.15462	0.76	0.73	0.03	17, 18, 19
49	2B11-1	95.0	2.0	M	35.0	13.003	0.15458	0.73	0.73	0	14
50	1909-261	59.8	3.1	M	35.3	13.004	0.15528	0.59	0.61	−0.02	13, 24
51	HEW-3	69.8	3.1	M	36.0	13.002	0.15500	0.65	0.65	0	6, 11
52	P2B	93.1	1.5	M	38.0	12.995	0.15460	0.75	0.73	0.02	4
53	GC-2	32.5	0.8	T	40.9	12.966	0.15605	0.55	0.55	0	9, 23
54	HEW-15	53.6	4.7	M	42.0	12.984	0.15537	0.63	0.62	0.01	6, 11
55	HEW-4	57.6	3.4	M	42.0	12.999	0.15529	0.60	0.63	−0.03	6, 11
56	HEW-5	67.7	5.3	M	43.0	12.998	0.15522	0.62	0.67	−0.05	6, 11
57	SP-C	90.5	1.1	M	43.6	12.996	0.15469	0.73	0.75	−0.02	17, 18, 19
58	P50-56	87.7	0.4	M	44.0	12.995	0.15465	0.74	0.74	0	26
59	BENSON	95.0	0.0	M	44.5	12.997	0.15451	0.76	0.76	0	26
60	FOX-86	79.0	5.0	M	45.0	12.996	0.15468	0.73	0.72	0.01	8
61	FOX-46	80.9	3.1	M	45.0	12.994	0.15465	0.74	0.72	0.02	8
62	PUYE	42.0	1.2	M	45.5	12.974	0.15566	0.60	0.60	0	26
63	SP-D	82.3	1.4	M	46.2	12.982	0.15488	0.73	0.73	0	17, 18, 19
64	FOX-18	81.7	2.7	M	48.0	12.994	0.15466	0.74	0.74	0	8
65	SP-F	74.5	1.5	M	49.0	12.976	0.15504	0.72	0.73	−0.01	17, 18, 19
66	FOX-82	77.9	5.4	M	49.0	12.994	0.15469	0.73	0.74	−0.01	8
67	P2A	93.1	1.5	M	49.0	12.989	0.15455	0.78	0.78	0	4
68	MT.GIBELE	22.3	6.9	T	49.2	12.936	0.15642	0.56	0.57	−0.01	10, 22
69	A1D	90.4	1.4	T	53.0	12.984	0.15453	0.81	0.79	0.02	4
70	439	44.1	3.9	M	53.3	12.993	0.15574	0.59	0.65	−0.06	13, 24
71	MAB177	0.3	0.0	T	53.6	—	—	0.58	0.55	0.03	21
72	SH1070	88.0	0.0	M	55.5	12.983	0.15458	0.79	0.79	0	6, 11
73	DQ-1	25.2	6.5	T	56.0	12.953	0.15625	0.54	0.62	−0.08	5

Table 3—*Continued*

No.	Sample	Or (mol%)	Non-alkali	Sym	$2V_x$ (°)	b (Å)	c^* (Å^{-1})	Σt_1 (b, c^*)	Σt_1 ($2V$, Or)	Δ	Ref
74	HEW-10	27.9	2.8	T	56.0	12.935	0.156 23	0.61	0.62	−0.01	6, 11
75	FOX-B	85.8	2.3	M	56.0	12.988	0.154 52	0.79	0.79	0	8
76	I-5	0.0	0.0	T	57.0	—	—	0.58	0.57	0.01	16
77	I-1	0.0	0.0	T	58.0	—	—	0.60	0.58	0.02	16
78	I-3B	0.0	0.0	T	58.0	—	—	0.59	0.58	0.01	16
79	CA1A	88.6	1.9	M	60.0	12.984	0.154 48	0.81	0.82	−0.01	4
80	FOX-C	88.9	1.4	M	60.0	12.976	0.154 43	0.84	0.82	0.02	8
81	HIMALAYA	88.1	0.0	M	63.0	12.963	0.154 41	0.88	0.84	0.04	15
82	SP-V	88.0	1.4	M	63.5	12.973	0.154 50	0.84	0.84	0	17, 18, 19
83	FOX-D	88.1	1.0	M	64.0	12.971	0.154 43	0.85	0.85	0	8
84	7007	88.1	1.0	M	65.0	12.967	0.154 51	0.85	0.85	0	13
85	CA1B	88.6	1.9	T	65.0	12.976	0.154 33	0.88	0.86	0.02	4
86	HEW-6	89.4	0.8	M	66.0	12.976	0.154 49	0.83	0.86	−0.03	6, 11
87	MAB169	0.3	0.0	T	66.1	—	—	0.64	0.64	0	21
88	MAB176	0.3	0.0	T	66.7	—	—	0.66	0.65	0.01	21
89	I-12	0.0	0.0	T	67.0	—	—	0.66	0.65	0.01	16
90	SP-B	89.0	1.3	M	68.5	12.970	0.154 39	0.87	0.88	−0.01	17, 18, 19
91	FOX-E	83.3	0.7	T	70.0	12.970	0.154 42	0.88	0.88	0	8
92	P1C	90.0	1.4	T	71.0	12.971	0.154 31	0.90	0.90	0	4
93	SP-Z	87.4	1.1	M	71.8	12.965	0.154 42	0.88	0.90	−0.02	17, 18, 19
94	SP-U	86.8	1.1	T	76.0	12.960	0.154 25	0.95	0.93	0.02	17, 18, 19
95	PONTISKALK	98.0	0.0	T	77.0	12.962	0.154 04	0.99	0.96	0.03	7
96	I-3A	0.0	0.0	T	78.0	—	—	0.79	0.75	0.04	16
97	RC20C	85.5	1.3	T	78.5	12.961	0.154 17	0.96	0.95	0.01	4
98	V-3	0.0	0.0	T	80.0	—	—	0.77	0.76	0.01	16
99	CA1E	88.6	1.9	T	82.0	12.963	0.154 08	0.98	0.98	0	4
100	PELLOTSALO	95.0	0.0	T	82.5	12.964	0.153 99	1.00	0.99	0.01	1
101	PRILEP	96.5	0.0	T	84.0	12.964	0.154 00	1.00	1.01	−0.01	20
102	MAB171	0.3	0.0	T	85.9	—	—	0.80	0.82	−0.02	21
103	III-16	0.0	0.0	T	92.0	—	—	0.92	0.88	0.04	16
104	MAB167	0.3	0.0	T	96.6	—	—	0.92	0.93	−0.01	21
105	MAB172A	0.3	0.0	T	97.4	—	—	0.93	0.94	−0.01	21
106	III-47	0.0	0.0	T	98.0	—	—	0.95	0.94	0.01	16
107	MAB151	0.3	0.0	T	98.8	—	—	0.95	0.95	0	21
108	TIBURON	0.3	0.0	T	102.5	12.781	0.156 53	0.99	0.99	0	22, 23
109	LA-CC	0.3	0.0	T	103.4	—	—	1.00	1.00	0	21

Note: For $2V$ values, a minus sign indicates that the optic axial plane is parallel to (010). Sym = symmetry (M = monoclinic, T = triclinic). $\Sigma t_1(b, c^*) = \Sigma t_1$ derived from observed b and c^* or other lattice parameters or diffraction peak positions (see text). $\Sigma t_1(2V, Or) = \Sigma t_1$ estimated from $2V$ and mole percent Or using Figure 2. $\Delta = \Sigma t_1(b, c^*) - \Sigma t_1(2V, Or)$. References are follows: (1) Bailey, 1969. (2) Brown and Bailey, 1964. (3) Cole et al., 1949. (4) DePieri, 1979. (5) DePieri and Quareni, 1973. (6) Emerson and Guidotti, 1974. (7) Finney and Bailey, 1964. (8) Fox and Moore, 1969. (9) Gering, 1985. (10) Harlow, 1982. (11) Hewlett, 1959. (12) Ott, 1982. (13) Phillips and Ribbe, 1973. (14) Priess, 1981. (15) Prince et al., 1973. (16) Raase and Kern, 1969. (17) Smith and Ribbe, 1966. (18) Spencer, 1937. (19) Stewart and Wright, 1974. (20) Strob, 1983. (21) Su et al., 1986a. (22) Su, 1986. (23) Wainwright and Starkey, 1969. (24) Warner et al., 1984. (25) Weitz, 1972. (26) Wright and Stewart, 1968. (27) Zeipert and Wondratschek, 1981.

structural state (Table 1). The calculations used in constructing this diagram are given in detail in Appendix 1, as is the derivation of the following equation relating Σt_1 to V_X, one-half the optic axial angle $2V_X$, and to X_{Or}, the mole fraction (*not* mole percent) of $KAlSi_3O_8$:

$$\Sigma t_1 = \frac{b_0 + b_1 X_{Or} + b_2 X_{Or} \sin^2 V_X + b_3 \sin^2 V_X}{a_0 + a_1 X_{Or} + a_2 X_{Or} \sin^2 V_X + a_3 \sin^2 V_X}. \quad (1)$$

Because a two-segment linear model was adopted for the variation of refractive indices with Or content and two different orientations of optic axial plane exist for K-rich members, three sets of coefficients for Equation 1 are required to account for the three cases: (A) where Or ≤ 60 mol% ($X_{Or} \leq 0.6$), (B) where Or > 60 mol% ($X_{Or} > 0.6$) and O.A.P. is approximately ⊥ (010), and (C) where Or > 60 mol% ($X_{Or} > 0.6$) and O.A.P. = (010). The coefficients are listed in Table 2. The reason that X_{Or} is used in Equation 1 instead of mole percent Or is so that the coefficients a_1, a_2 and b_1, b_2 have about the same magnitudes as the other coefficients. If X_{Or} is replaced by mole percent Or in Equation 1, the values of a_1, a_2 and b_1, b_2 in the abstract and in Table 2 should be divided by 100.

For those who are undertaking systematic investigation of the structural states of alkali feldspars in certain geologic terranes, Equation 1 should prove useful if a computer is employed to process the experimental data.

Evaluation of the determinative diagram

Data for a total of 109 natural, heated natural, and synthetic alkali feldspars are plotted in Figure 2 and are listed in Table 3 together with their compositions, measured $2V_X$ angles, selected lattice parameters (where available), and structural states as expressed by Σt_1, the total Al content of the two T_1 tetrahedral sites. Values of Σt_1 are, of course, model-dependent, and this has been reviewed in detail by Kroll and Ribbe (1983). The now familiar b-c plot of Wright and Stewart (1968) has been used for more than 15 years to obtain estimates of Σt_1 for

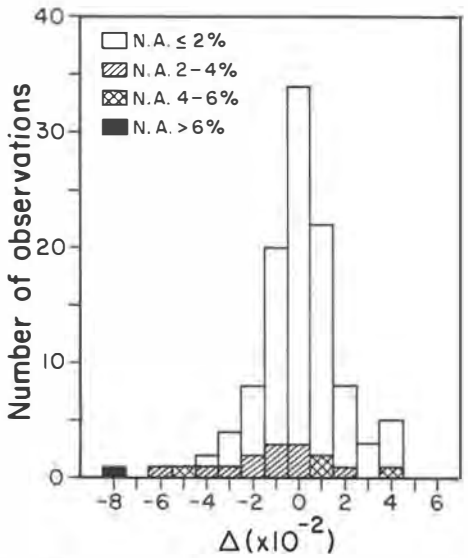

Fig. 3. Histogram showing frequency distribution of Δ values from Table 2: N.A. (non-alkali) refers to the mole percentage of endmembers other than Ab and Or.

alkali feldspars, but there has always been a flaw in its use: plots of b versus c for alkali-exchange series are nonlinear, leading to systematic misestimates in Σt_1 of up to 0.05 (see, e.g., Luth, 1974; Hovis, 1984).

Recently Kroll and Ribbe (in prep.) have found that a plot of b versus c^* for the alkali-exchange series is linear (to within about 0.01 in Σt_1) and parallel to Σt_1 contours on a b-c^* quadrilateral. They have derived equations for determining Σt_1 based on crystal-structure analyses of 21 monoclinic and 16 triclinic alkali feldspars and a different algorithm for calculating Σt_1 from lattice-parameter data. For monoclinic feldspars,

$$\Sigma t_1 = 2t_1 = 72.245 - 3.1130b - 200.785c^*. \quad (2)$$

For triclinic feldspars,

$$\Sigma t_1 = t_1o + t_1m = \frac{b - 21.5398 + 53.8405c^*}{21.1567 - 15.8583c^*}. \quad (3)$$

We used these equations to calculate Σt_1 for the 93 samples in Table 3 whose unit-cell dimensions were known.

For the eight intermediate synthetic albites studied by Raase and Kern (1969), Σt_1 was calculated using their reported values of $\Delta 131 \equiv 2\theta(131) - 2\theta(1\bar{3}1)$ for Cu$K\alpha$ radiation and the equation $\Sigma t_1 = t_1o + (1 - t_1o)/3$, where $t_1o = 1.965 - 0.849(\Delta 131)$ and where $(1 - t_1o)/3 = t_1m = t_2o = t_2m$ is implicitly assumed. Similar values for Σt_1 are given by Smith (1974, Fig. 8.7) in his interpretation of Raase and Kern's results. For the eight albite crystals in the Clear Creek series, Σt_1 values were calculated using reciprocal lattice angles α^* and γ^*, as described by Su et al. (1986a, Eqs. 2 and 4).

An estimated Al content of the T_1 tetrahedral sites, $\Sigma t_1(2V,Or)$ was obtained for each sample in Table 3 from its $2V_X$ value and composition relative to the Σt_1 contours in Figure 2. Nearly 83% of the Σt_1 values are within ±0.02 of Σt_1 calulated from lattice parameters, and 97% are within ±0.04 (cf. Fig. 3). This remarkable agreement substantiates the linear model for variation of refractive indices in the series LA–HA and LM–HS and the two-segment models for HA–HS and LA–LM. In particular it justifies the choices of $2V_X$ and refractive indices for the hypothetical endmembers and for Or_{60} of low and high structural state. And one can conclude from this test that the standard error for estimating Σt_1 from $2V$ and Or content by using this diagram is about 0.02, which is the same as that attained by various models that rely on refined lattice parameters or reflection peak positions from X-ray powder-diffraction data, e.g., b-c, b-c^*, $2\theta(060)$-$2\theta(\bar{2}04)$ methods, etc.

Also marked in Figure 3 are the numbers of samples containing totals of >2mol% non-alkali feldspar components. It seems that high non-alkali content tends to cause an underestimate of Σt_1 if we treat the Σt_1 estimated from lattice parameters b and c^* as the "true" values. This may be due to the fact that $\Sigma t_1 > 1.00$ in feldspars with An, Cn, and Srf components.

It should be recalled that the final $2V_X$ values (and thus the refractive indices) for hypothetical LM and HS and the Or_{60} reference points were adjusted a few degrees one way or the other to attain a best fit of the model to the *entire* data set, and this represents one degree of empiricism inherent in the present model. The others are the models relating lattice parameters to Σt_1 and for that matter, those relating results of crystal-structure analyses, i.e., (Al,Si)–O bond lengths, to lattice parameters. Further refinement of Figure 2 for use in determining structural states may be anticipated as new, more precise data become available, but for the moment this diagram should prove very useful in routine petrographic investigations of natural, alkali-exchanged, heat-homogenized alkali feldspars. On the other hand, it may also be reasonably anticipated that, even if there are refinements, the actual adjustments will be relatively minor, because most of the samples used in evaluating this model are representative of alkali feldspars in terms of their geologic occurrences, or conditions of formation, and their ranges of chemical composition, including both major and minor constituents.

Case study of alkali-exchange series

Wright and Stewart (1968) described six alkali-exchange series. For each they measured $2V_X$ and the unit-cell parameters on (1) a starting material of known composition, (2) its K-exchanged equivalent, and (3) its Na-exchanged equivalent. They estimated compositions of exchanged materials from unit-cell volumes (see Table 4). We calculated $\Sigma t_1(b, c^*)$ from the b and c^* lattice parameters, using Equations 2 and 3 above. Note in the far right column of Table 5 that structural state does not vary significantly [±0.02 in Σt_1] among any three members of a series, indicating that the (Al,Si) distribution has remained almost unaffected during the exchange experiments. This is an expected result, and one that has been demonstrated in dozens of similar experiments.

For the five sanidine and orthoclase specimens, the mean

Table 4. Compositional, optical, and structural state data for six feldspars that were alkali-exchanged by Wright and Stewart (1968)

Sample	Or (mol%)	$2V_x$ (°)			$\Sigma t_1(2V, Or)$			Σt_1 (b, c^*)
		Min	Max	Mean	Min	Max	Mean	
Puye sanidine	42	40.5	49.0	45.5	0.57	0.62	0.60	0.60
Puye sanidine + KCl	95	−52.0	19.0	−17.0	0.55	0.70	0.63	0.61
Puye sanidine + NaCl	2	42.5	52.0	48.0	0.50	0.54	0.52	0.62
P50-56 orthoclase	86	41.5	52.0	44.5	0.72	0.77	0.74	0.74
P50-56 orthoclase + KCl	95	35.0	42.0	39.0	0.73	0.75	0.74	0.74
P50-56 orthoclase + NaCl	8	61.5	67.0	65.0	0.62	0.66	0.65	0.71
Benson orthoclase	95	37.5	51.5	44.5	0.74	0.79	0.76	0.76
Benson orthoclase + NaCl + KCl	97	38.5	45.5	42.0	0.74	0.77	0.75	0.76
Benson orthoclase + NaCl	7	64.0	67.0	66.0	0.64	0.67	0.66	0.72
SH1070 orthoclase	88	50.0	60.0	55.5	0.77	0.82	0.80	0.79
SH1070 orthoclase + KCl	96	48.0	48.5	48.0	0.78	0.78	0.78	0.79
SH1070 orthoclase+ NaCl	4	66.5	74.5	69.5	0.65	0.72	0.68	0.76
Spencer-B orthoclase	89			68.4			0.87	0.87
Spencer-B orthoclase + NaCl	11	72.5	77.0	75.0	0.72	0.76	0.74	0.85
Spencer-U microcline	84	69.0	72.0	71.0	0.87	0.89	0.88	0.95
Spencer-U microcline + KCl	94	67.5	71.0	70.0	0.88	0.91	0.90	0.94
Spencer-U microcline + NaCl	0	78.5	86.0	82.5	0.75	0.82	0.79	0.96

Note: The range and the mean value of $2V_x$ for each sample and the corresponding Σt_1 values estimated from Figure 2 using $2V_x$ and Or are listed. These are compared to Σt_1 estimated from lattice parameters b and c^*, using Equations 2 and 3.

values of $\Sigma t_1(2V, Or)$, i.e., those determined from $2V$ and mole percent Or using Figure 2, agree within ±0.02 with $\Sigma t_1(b, c^*)$ for the natural and K-exchanged specimens only. For all the Na-exchanged members, however, mean $\Sigma t_1(2V, Or)$ is systematically less than $\Sigma t_1(b, c^*)$ by 0.06 to as much as 0.11. A possible explanation for these discrepancies is the fact that the starting material is monoclinic and the Na-exchanged member triclinic. By analogy with the sanidine-microcline transformation, one might expect polysynthetic albite and/or pericline twins to develop with inversion. If the Na-exchanged member is submicroscopically twinned, the optical properties will be different from its untwinned equivalent (Marfunin, 1966, Table 21, p. 140; see also Smith, 1974, Table 8-1, p. 372).

With a program by Hauser and Wenk (1976) as modified by B. J. Cooper, we calculated the effects of both submicroscopic albite and pericline twinning on $2V_X$ of albite using the refractive indices and optic orientation of a high albite ($\Sigma t_1 = 0.59$, specimen MAB-177 described by Su et al., 1986b, Table 1). The results in Table 5 indicate that $2V_X$ could be reduced by up to 20°, implying that a crystal is more disordered than it actually is, depending on the degree and type or mix of types of submicroscopic twinning.

Table 5. Effects of submicroscopic twinning on $2V_x$ (in degrees) of high albite

Twin law	Host	Ab	Pe	Ab-Pe	$2V_x$	$\Delta(2V_x)$
None	100	0	0	0	53.6	0.0
Albite	90	10	0	0	49.2	4.4
	80	20	0	0	44.5	9.1
	70	30	0	0	39.5	14.1
	60	40	0	0	35.1	18.5
	50	50	0	0	33.2	20.4
Pericline	90	0	10	0	49.8	3.8
	80	0	20	0	45.9	7.7
	70	0	30	0	42.1	11.5
	60	0	40	0	39.2	14.4
	50	0	50	0	38.0	15.6
Albite-pericline	40	40	10	10	35.1	18.5
	30	30	20	20	36.9	16.7
	25	25	25	25	37.8	15.8

Note: The host material is MAB-177, a high albite with $\Sigma t_1 = 0.59$ (see Su et al., 1986a, Table 1). Host = percentage of untwinned host individual; Ab = percentage of albite-law twin individual; Pe = percentage of pericline-law twin individual; Ab-Pe = percentage of albite-pericline–law twin individual. $\Delta(2V_x)$ is the difference between the $2V_x$ of untwinned crystal and that of twinned crystal.

The fact that the original Spencer U specimen is not homogeneous but contains two phases (Stewart and Wright, 1974) may have some bearing on the confusion surrounding this specimen.

This "comfortable" conclusion is, however, open to question, because the intermediate microcline (Spencer U, Table 4), that started as triclinic and presumably is no more twinned *after* Na-exchange than *before*, also shows too low a $2V_X$ value and thus appears to be significantly more disordered than is indicated by $\Sigma t_1(b, c^*)$. Of course, additional twinning may have been introduced by the exchange process. Even for unexchanged and K-exchanged Spencer U, note that there is poor agreement between $\Sigma t_1(2V, Or)$ [= 0.88, 0.90] and $\Sigma t_1(b, c^*)$ [= 0.95] and that the $\Sigma t_1(b, c^*)$ value is further than the $\Sigma t_1(2V, Or)$ value from $\Sigma t_1 = 0.91$ calculated by Kroll and Ribbe (1983, Table 3, p. 65) from a structural analysis by Bailey (1969).

Acknowledgments

This work was supported in part by National Science Foundation Grant EAR 83-08308 to F.D.B. and P.H.R. S.C.S. gratefully acknowledges financial support from N.S.F. and a Cunningham Fellowship awarded by Virginia Polytechnic Institute and State University. Prof. H. Wondratschek of Universität Karlsruhe, West Germany, and especially Dr. D. B. Stewart of the U.S. Geological Survey, Reston, Virginia, provided many constructive comments during the course of this research. We thank B. J. Cooper, Sam Houston State University, Huntsville, Texas, for providing the modified Hauser-Wenk program.

References

Bailey, S.W. (1969) Refinement of an intermediate microcline structure. American Mineralogist, 54, 1540–1545.

Bambauer, H.U., Taborszky, F., and Trochim, H.D. (1979) Optical determination of rock-forming minerals. Part 1. Determinative tables. Schweizerbart'sche Verlagsbuchhandlung, Stuttgart, 188 p.

Bertelmann, D., Förtsch, E., and Wondratschek, H. (1985) Zum Temperverhalten von Sanidinen: Die Ausnahmerolle der Eifelsanidin-Megakristalle. Neues Jahrbuch für Mineralogie, Abhandlungen, 152, 123–141.

Blasi, A., DePol Blasi, C., and Zanazzi, P.F. (1985) Pellotsalo maximum low microcline: Its structure re-refinement and mineralogical implications. European Union of Geosciences Meeting III, Strasbourg, France, April 1–14, 1985, Program with Abstracts, V26.

Bloss, F.D. (1985) Labelling refractive index curves for mineral series. American Mineralogist, 70, 428–432.

Brown, B.E., and Bailey, S.W. (1964) The structure of maximum microcline. Acta Crystallographica, 17, 1391–1400.

Burri, C., Parker, R.L., and Wenk, E. (1967) Die optische Orientierung der Plagioklase—Unterlagen und Diagramme zur Plagioklase-bestimmung nach der Drehtische-methode. Birkhäuser, Basel und Stuttgart, 334 p.

Cole, W.F., Sörum, H., and Kennard, O. (1949) The crystal structures of orthoclase and sanidinized orthoclase. Acta Crystallographica, 2, 280–287.

Crawford, M.L. (1966) Composition of plagioclase and associated minerals in some schists from Vermont, U.S.A., and South Westland, New Zealand, with inferences about the peristerite solvus. Contributions to Mineralogy and Petrology, 13, 269–294.

DePieri, R. (1979) Cell dimensions, optic axial angle and structural state in triclinic K-feldspar of the Adamello massif, northern Italy. Memorie de Scienze Geologiche, Padova, 32.

DePieri, R., and Quareni, S. (1973) The crystal structure of an anorthoclase: An intermediate alkali feldspar. Acta Crystallographica, B29, 1483–1487.

Emerson, R.W., and Guidotti, C.F. (1974) New X-ray and chemical data on Hewlett's 1959 feldspar suite. American Mineralogist, 59, 615–617.

Finney, J.J., and Bailey, S.W. (1964) Crystal structure of an authigenic maximum microcline. Zeitschrift für Kristallographie, 119, 413–436.

Fox, P.E., and Moore, J.M., Jr. (1969) Feldspars from Adamant pluton, British Columbia. Canadian Journal of Earth Sciences, 6, 1199–1209.

Gering, E. (1985) Silizium/Aluminium-Ordnung und Kristallperfektion von Sanidinen. Dissertation, Universität Karlsruhe.

Harlow, G.E. (1982) The anorthoclase structures: The effects of temperature and composition. American Mineralogist, 67, 975–996.

Harlow, G.E., and Brown, G.E., Jr. (1980) Low albite: An X-ray and neutron diffraction study. American Mineralogist, 65, 986–995.

Hauser, J., and Wenk, H.-R. (1976) Optical properties of composite crystals (submicroscopic domains, exsolution lamellae, solid solution). Zeitschrift für Kristallographie, 143, 188–219.

Hewlett, C.G. (1959) Optical properties of potassic feldspars. Geological Society of America Bulletin, 70, 511–538.

Hovis, G.L. (1984) Characterization of Al-Si distributions in alkali feldspars. Geological Society of America Abstracts with Programs, 16, 544.

Kroll, H., and Ribbe, P.H. (1983) Lattice parameters, composition and (Al,Si) order in alkali feldspars. Mineralogical Society of America Reviews in Mineralogy, 2, 2nd edition, 57–100.

Laves, F., and Chaisson, U. (1950) An X-ray investigation of the "high"-"low" albite relations. Journal of Geology, 58, 584–592.

Luth, W.C. (1974) Analysis of experimental data on alkali feldspars: Unit cell parameters and solvi. In W.S. MacKenzie and J. Zussman, Eds. The feldspars, 249–296. Manchester University Press, Manchester.

Marfunin, A.S. (1966) The feldspars: Phase relations, optical properties, and geological distribution. (Transl. from the Russian edition, 1962.) Israel Program for Scientific Translations, Jerusalem, 317 p.

Orville, P.M. (1967) Unit-cell parameters of the microcline–low albite and the sanidine–high albite solid solution series. American Mineralogist, 52, 55–86.

Ott, G. (1982) Röntgenographische Strukturverfeinerungen an getemperten Eifelsanidinen zur Feststellung ihres Ordnungszustandes. Diplomarbeit, Universität Karlsruhe, West Germany.

Phillips, M.W., and Ribbe, P.H. (1973) The structures of monoclinic potassium-rich feldspars. American Mineralogist, 58, 263–270.

Plas, L. van der (1966) The identification of detrital feldspars. Elsevier, Amsterdam, 305 p.

Priess, U. (1981) Untersuchungen zur Tief-Hoch-Umwandlung von Fe-hältigen Orthoklas-Kristallen aus Madagascar. Neues Jahrbuch für Mineralogie, Abhandlungen, 141, 17–29.

Prince, E., Donnay, G., and Martin, R.F. (1973) Neutron diffraction refinement of an ordered orthoclase structure. American Mineralogist, 58, 500–507.

Raase, P., and Kern, H. (1969) Über die Synthese von Albiten bei Temperaturen von 250 bis 700°C. Contributions to Mineralogy and Petrology, 21, 225–237.

Rankin, D.W. (1967) Axial angle determinations in Orville's microcline–low albite solid solution series. American Mineralogist, 52, 414–417.

Schneider, T.R. (1957) Röntgenographic und optische Untersuchung der Um wandung. Albit-Analbit-Monalbit. Zeitschrift für Kristallographie, 109, 245–271.

Smith, J.R. (1958) Optical properties of heated plagioclases. American Mineralogist, 43, 1179–1194.

Smith, J.V. (1974) Feldspar minerals. I. Crystal structure and physical properties. Springer-Verlag, Heidelberg, 672 p.

Smith, J.V., and Ribbe, P.H. (1966) X-ray-emission microanalysis of rock-forming minerals. III. Alkali feldspars. Journal of Geology, 76, 197–216.

Spencer, E. (1937) The potash-feldspars I. Thermal stability. Mineralogical Magazine, 24, 453–494.

Stewart, D.B. (1974) Optic axial angle and extinction angles of alkali feldspars related by cell parameters to Al/Si order and composition. In W.S. MacKenzie and J. Zussman, Eds. The feldspars, 145–161. Manchester University Press, Manchester.

Stewart, D.B., and Ribbe, P.H. (1969) Structural explanation for variations in cell parameters of alkali feldspar with Al/Si ordering. American Journal of Science, 267-A, 144–462.

——— (1983) Optical properties of feldspars. Mineralogical Society of America Reviews in Mineralogy, 2, 2nd Edition, 121–139.

Stewart, D.B., and Wright, T.L. (1974) Al/Si order and symmetry of natural alkali feldspars, and the relationship of strained cell parameters to bulk composition. Bulletin de la Société française de Minéralogie et de Cristallographie, 97, 356–377.

Strob, W. (1983) Strukturverfeinerung eines Tief-Mikroklins, Zusammenhange zwischen <T–O> Abstanden und (Al,Si)-Ordnungsgrad und metrische Variation in einer Tief-Albit/Tief-Mikroklin-Mischkristallreihe. Diplomarbeit, Westfälische Wilhelms-Universität, Münster, West Germany.

Su, S.C. (1986) Alkali feldspars: Ordering, composition and optical properties. Ph.D. dissertation, Virginia Polytechnic Institute and State University, Blacksburg.

Su, S.C., Bloss, F.D., Ribbe, P.H., and Stewart, D.B. (1984) Optic axial angle, a precise measure of (Al,Si) ordering in T_1 tetrahedral sites of K-rich alkali feldspars. American Mineralogist, 69, 440–448.

Su, S.C., Ribbe, P.H., Bloss, F.D., and Goldsmith, J.R. (1985) Structural states and properties of a low-high albite series of single crystals. Geological Society of America Abstracts with Programs, 17, 729.

Su, S.C., Ribbe, P.H., Bloss, F.D., and Goldsmith, J.R. (1986a) Optical properties of single crystals in the order-disorder series low albite–high albite. American Mineralogist, 71, 1384–1392.
Su, S.C., Ribbe, P.H., Bloss, F.D., and Warner, J.K. (1986b) Optical properties of a high albite–high sanidine solid-solution series. American Mineralogist, 71, 1393–1398.
Tuttle, O.F. (1952) Optical studies on alkali feldspars. American Journal of Science, Bowen volume, 553–568.
Tuttle, O.F., and Bowen, N.L. (1958) Origin of granite in light of experimental studies in the system $NaAlSi_3O_8$-$KAlSi_3O_8$-SiO_2-H_2O. Geological Society of America Memoir 74, 153 p.
Wainwright, J.E.N., and Starkey, J. (1969) Crystal structure of a metamorphic low albite. (abs.) Geological Society of America Special Paper 121, 310.
Warner, J.K., Su, S.C., Ribbe, P.H., and Bloss, F.D. (1984) Optical properties of the analbite–high sanidine solid solution series. Geological Society of America Abstracts with Programs, 16, 687.
Weitz, G. (1972) Die Struktur des Sanidins bei verschiedenen Ordnungsgraden. Zeitschrift für Kristallographie, 136, 418–426.
Wolfe, H.E. (1976) Optical and X-ray study of the low plagioclases. M.S. thesis, Virginia Polytechnic Institute and State University. Blacksburg.
Wright, T.L. (1968) X-ray and optical study of alkali feldspars: II. An X-ray method for determining the composition and structural state from measurement of 2θ values for three reflections. American Mineralogist, 53, 88–104.
Wright, T.L., and Stewart, D.B. (1968) X-ray and optical study of alkali feldspars: I. Determination of compositions and structural state from refined unit-cell parameters and $2V$. American Mineralogist, 53, 38–87.
Zeipert, C., and Wondratschek, H. (1981) Ein ungewöhnliches Temperverhalten bei Sanidin von Volkesfeld/Eifel. Neues Jahrbuch für Mineralogie Monatshefte, 407–415.

Manuscript received April 23, 1986
Manuscript accepted August 6, 1986

Appendix 1. Calculation of $2V$-Or diagram contoured for Σt_1

Because a two-segment linear model with inflection point at Or_{60} was used to delineate the variations of refractive indices of alkali feldspar series with the same structural state, calculations were carried out separately for the ranges Or_0–Or_{60} and Or_{60}–Or_{100}. For the latter, two orientations of the optic axial plane (O.A.P.) were also treated separately. The refractive indices of endmembers and Or_{60} members are those listed in Table 1. Symbols used in the following derivations are Or = mole percent $KAlSi_3O_8$ (X_{or} = Or/100); Σt_1 = Al content of T_1 sites; and A, B, C = principal refractive indices most nearly parallel to crystallographic directions **a**, **b**, **c**, respectively, at given Σt_1 and Or. In the following equations, superscripts indicate the values of Σt_1, and subscripts the values of mole percent Or. E.g., ${}^{0.6}(n_a)_{60}$ is n_a at $\Sigma t_1 = 0.6$ and Or = 60, and ${}^{1.0}(n_b)_{Or}$ is n_b at $\Sigma t_1 = 1.0$ and given Or.

Case A: Or ≤ 60

1. Refractive indices for the series with $\Sigma t_1 = 1.0$.

$$ {}^{1.0}(n_a)_{Or} = {}^{1.0}(n_a)_0 + ({}^{1.0}(n_a)_{60} - {}^{1.0}(n_a)_0)Or/60, \quad (A1) $$
$$ {}^{1.0}(n_b)_{Or} = {}^{1.0}(n_b)_0 + ({}^{1.0}(n_b)_{60} - {}^{1.0}(n_b)_0)Or/60, \quad (A2) $$
$$ {}^{1.0}(n_c)_{Or} = {}^{1.0}(n_c)_0 + ({}^{1.0}(n_c)_{60} - {}^{1.0}(n_c)_0)Or/60. \quad (A3) $$

2. Refractive indices for the series with $\Sigma t_1 = 0.6$.

$$ {}^{0.6}(n_a)_{Or} = {}^{0.6}(n_a)_0 + ({}^{0.6}(n_a)_{60} - {}^{0.6}(n_a)_0)Or/60, \quad (A4) $$
$$ {}^{0.6}(n_b)_{Or} = {}^{0.6}(n_b)_0 + ({}^{0.6}(n_b)_{60} - {}^{0.6}(n_b)_0)Or/60, \quad (A5) $$
$$ {}^{0.6}(n_c)_{Or} = {}^{0.6}(n_c)_0 + ({}^{0.6}(n_c)_{60} - {}^{0.6}(n_c)_0)Or/60. \quad (A6) $$

3. Refractive indices at Σt_1 and Or.

$$ A = {}^{\Sigma t_1}(n_a)_{Or} = {}^{1.0}(n_a)_{Or} - ({}^{0.6}(n_a)_{Or} - {}^{1.0}(n_a)_{Or})(\Sigma t_1 - 1.0)/0.4, \quad (A7) $$
$$ B = {}^{\Sigma t_1}(n_b)_{Or} = {}^{1.0}(n_b)_{Or} - ({}^{0.6}(n_b)_{Or} - {}^{1.0}(n_b)_{Or})(\Sigma t_1 - 1.0)/0.4, \quad (A8) $$
$$ C = {}^{\Sigma t_1}(n_c)_{Or} = {}^{1.0}(n_c)_{Or} - ({}^{0.6}(n_c)_{Or}) - {}^{1.0}(n_c)_{Or})(\Sigma t_1 - 1.0)/0.4. \quad (A9) $$

4. Optic axial angle $2V_X$ at Σt_1 and Or.

$$ 2V_X = 2\sin^{-1}\sqrt{(C^{-2} - B^{-2})/(A^{-2} - B^{-2})}. \quad (A10) $$

Case B: Or > 60 and O.A.P. (~) ⊥ (010)

1. Refractive indices for the series with $\Sigma t_1 = 1.0$.

$$ {}^{1.0}(n_a)_{Or} = {}^{1.0}(n_a)_{60} + ({}^{1.0}(n_a)_{100} - {}^{1.0}(n_a)_{60})(Or - 60)/40, \quad (A11) $$
$$ {}^{1.0}(n_b)_{Or} = {}^{1.0}(n_b)_{60} + ({}^{1.0}(n_b)_{100} - {}^{1.0}(n_b)_{60})(Or - 60)/40, \quad (A12) $$
$$ {}^{1.0}(n_c)_{Or} = {}^{1.0}(n_c)_{60} + ({}^{1.0}(n_c)_{100} - {}^{1.0}(n_c)_{60})(Or - 60)/40. \quad (A13) $$

2. Refractive indices for the series with $\Sigma t_1 = 0.6$.

$$ {}^{0.6}(n_a)_{Or} = {}^{0.6}(n_a)_{60} + ({}^{0.6}(n_a)_{100} - {}^{0.6}(n_a)_{60})(Or - 60)/40, \quad (A14) $$
$$ {}^{0.6}(n_b)_{Or} = {}^{0.6}(n_b)_{60} + ({}^{0.6}(n_b)_{100} - {}^{0.6}(n_b)_{60})(Or - 60)/40, \quad (A15) $$
$$ {}^{0.6}(n_c)_{Or} = {}^{0.6}(n_c)_{60} + ({}^{0.6}(n_c)_{100} - {}^{0.6}(n_c)_{60})(Or - 60)/40. \quad (A16) $$

3. Refractive indices at Σt_1 and Or.

$$ A = {}^{\Sigma t_1}(n_a)_{Or} = {}^{1.0}(n_a)_{Or} - ({}^{0.6}(n_a)_{Or} - {}^{1.0}(n_a)_{Or})(\Sigma t_1 - 1.0)/0.4, \quad (A17) $$
$$ B = {}^{\Sigma t_1}(n_b)_{Or} = {}^{1.0}(n_b)_{Or} - ({}^{0.6}(n_b)_{Or} - {}^{1.0}(n_b)_{Or})(\Sigma t_1 - 1.0)/0.4, \quad (A18) $$
$$ C = {}^{\Sigma t_1}(n_c)_{Or} = {}^{1.0}(n_c)_{Or} - ({}^{0.6}(n_c)_{Or} - {}^{1.0}(n_c)_{Or})(\Sigma t_1 - 1.0)/0.4. \quad (A19) $$

4. Optic axial angle $2V_X$ at Or and Σt_1.

$$ 2V_X = 2\sin^{-1}\sqrt{(C^{-2} - B^{-2})/(A^{-2} - B^{-2})}. \quad (A20) $$

Case C: Or > 60 and O.A.P. = (010)

In this case, the equations for A, B, and C have the same forms as A17, A18, and A19, respectively, but $C > B$. Thus,

$$ 2V_X = 2\sin^{-1}\sqrt{(B^{-2} - C^{-2})/(A^{-2} - C^{-2})}. \quad (A21) $$

The above calculations were undertaken at increments of 1 mol% Or from 0 to 100 and for Σt_1 at increments of 0.01 from 0.5 to 1.0 to get $2V_X$ values at each (Or, Σt_1) point. Then $2V_X$ was plotted versus mole percent Or and contoured for Σt_1, as seen in Figure 2.

Derivation of Equation 1 in the text

Case A: Or ≤ 60

Substituting Equations A1 and A4 into A7, A2 and A5 into A8, A3 and A6 into A9, we can express the three principal refractive indices A, B, and C as functions of Σt_1 and Or:

$$ A = f_1(\Sigma t_1, Or), \quad (A22) $$
$$ B = f_2(\Sigma t_1, Or), \quad (A23) $$
$$ C = f_3(\Sigma t_1, Or). \quad (A24) $$

Because the birefringences of alkali feldspars are very low (≤0.011), the following approximate equation for calculating $2V$ from refractive indices can be used:

$$ \sin^2 V_X = (B - C)/(B - A). \quad (A25) $$

Substituting A22, A23, and A24 into A25 and rearranging the terms, we can express Σt_1 as a function of $\sin^2 V_X$ and X_{Or}.

$$\Sigma t_1 = \frac{b_0 + b_1 X_{Or} + b_2 X_{Or}\sin^2 V_X + b_3 \sin^2 V_X}{a_0 + a_1 X_{Or} + a_2 X_{Or}\sin^2 V_X + a_3 \sin^2 V_X}, \quad \text{(A26)}$$

where

$$\begin{aligned}
a_0 &= {}^{0.6}(n_c)_0 - {}^{1.0}(n_c)_0 - {}^{0.6}(n_b)_0 + {}^{1.0}(n_b)_0,\\
a_1 &= 5/3[({}^{0.6}(n_c)_{60} - {}^{0.6}(n_c)_0) - ({}^{0.6}(n_b)_{60} - {}^{0.6}(n_b)_0) - ({}^{1.0}(n_c)_{60}\\
&\quad - {}^{1.0}(n_c)_0) + ({}^{1.0}(n_b)_{60} - {}^{1.0}(n_b)_0)],\\
a_2 &= 5/3[({}^{1.0}(n_a)_{60} - {}^{1.0}(n_a)_0) - ({}^{1.0}(n_b)_{60} - {}^{1.0}(n_b)_0)\\
&\quad - ({}^{0.6}(n_a)_{60} - {}^{0.6}(n_a)_0) + ({}^{0.6}(n_b)_{60} - {}^{0.6}(n_b)_0)],\\
a_3 &= {}^{1.0}(n_a)_0 - {}^{0.6}(n_a)_0 - {}^{1.0}(n_b)_0 + {}^{0.6}(n_b)_0,\\
b_0 &= a_0 + 2/5({}^{1.0}(n_c)_0 - {}^{1.0}(n_b)_0),\\
b_1 &= a_1 + 2/3[({}^{1.0}(n_c)_{60} - {}^{1.0}(n_c)_0) - ({}^{1.0}(n_b)_{60} - {}^{1.0}(n_b)_0)],\\
b_2 &= a_2 + 2/3[({}^{1.0}(n_b)_{60} - {}^{1.0}(n_b)_0) - ({}^{1.0}(n_a)_{60} - {}^{1.0}(n_a)_0)],\\
b_3 &= a_3 + 2/5({}^{1.0}(n_b)_0 - {}^{1.0}(n_a)_0).
\end{aligned}$$

Case B: Or > 60 and O.A.P. (~) ⊥ (010)

In this case, the equation has the same form as A26, but the coefficients are different.

$$\begin{aligned}
a_0 &= {}^{0.6}(n_c)_{60} - {}^{0.6}(n_b)_{60} - {}^{1.0}(n_c)_{60} + {}^{1.0}(n_b)_{60} + 2/3[({}^{0.6}(n_c)_{60}\\
&\quad - {}^{0.6}(n_c)_{100}) - ({}^{0.6}(n_b)_{60} - {}^{0.6}(n_b)_{100}) - ({}^{1.0}(n_c)_{60} - {}^{1.0}(n_c)_{100})\\
&\quad + ({}^{1.0}(n_b)_{60} - {}^{1.0}(n_b)_{100})],\\
a_1 &= 5/2[({}^{0.6}(n_c)_{60} - {}^{0.6}(n_c)_{100}) - ({}^{0.6}(n_b)_{60} - {}^{0.6}(n_b)_{100}) - ({}^{1.0}(n_c)_{60}\\
&\quad - {}^{1.0}(n_c)_{100}) + ({}^{1.0}(n_b)_{60} - {}^{1.0}(n_b)_{100})],\\
a_2 &= {}^{0.6}(n_b)_{60} - {}^{0.6}(n_a)_{60} - {}^{1.0}(n_b)_{60} + {}^{1.0}(n_a)_{60} + 2/3[({}^{0.6}(n_a)_{60}\\
&\quad - {}^{0.6}(n_a)_{100}) - ({}^{0.6}(n_b)_{60} - {}^{0.6}(n_b)_{100}) - {}^{1.0}(n_a)_{60} - {}^{1.0}(n_a)_{100})\\
&\quad + ({}^{1.0}(n_b)_{60} - {}^{1.0}(n_b)_{100})],\\
a_3 &= 5/2[({}^{0.6}(n_b)_{60} - {}^{0.6}(n_b)_{100}) - ({}^{0.6}(n_a)_{60} - {}^{0.6}(n_a)_{100})\\
&\quad - ({}^{1.0}(n_b)_{60} - {}^{1.0}(n_b)_{100}) + ({}^{1.0}(n_a)_{60} - {}^{1.0}(n_a)_{100})],\\
b_0 &= a_0 + 2/5({}^{1.0}(n_c)_{60} - {}^{1.0}(n_b)_{60}) + 3/5[({}^{1.0}(n_c)_{60} - {}^{1.0}(n_c)_{100})\\
&\quad - ({}^{1.0}(n_b)_{60} - {}^{1.0}(n_b)_{100})],\\
b_1 &= a_1 + ({}^{1.0}(n_b)_{60} - {}^{1.0}(n_b)_{100}) - ({}^{1.0}(n_c)_{60} - {}^{1.0}(n_c)_{100})],\\
b_2 &= a_2 + ({}^{1.0}(n_a)_{60} - {}^{1.0}(n_a)_{100}) - ({}^{1.0}(n_b)_{60} - {}^{1.0}(n_b)_{100})],
\end{aligned}$$

Case C: Or > 60 and O.A.P. = (010)

In this case also, the equation still has the same form as A26, but the coefficients are different.

$$\begin{aligned}
a_0 &= {}^{0.6}(n_b)_{60} - {}^{0.6}(n_c)_{60} - {}^{1.0}(n_b)_{60} + {}^{1.0}(n_c)_{60} + 2/3[({}^{0.6}(n_c)_{60}\\
&\quad - {}^{0.6}(n_c)_{100}) - ({}^{0.6}(n_b)_{60} - {}^{0.6}(n_b)_{100}) - ({}^{1.0}(n_c)_{60} - {}^{1.0}(n_c)_{100})\\
&\quad + (1.0(n_b)_{60} - {}^{1.0}(n_b)_{100})],\\
a_1 &= 5/2[({}^{0.6}(n_b)_{60} - {}^{0.6}(n_b)_{100}) - ({}^{0.6}(n_c)_{60} - {}^{0.6}(n_c)_{100})\\
&\quad - ({}^{1.0}(n_b)_{60} - {}^{1.0}(n_b)_{100}) + ({}^{1.0}(n_c)_{60} - {}^{1.0}(n_c)_{100})],\\
a_2 &= 5/2[({}^{0.6}(n_c)_{60} - {}^{0.6}(n_c)_{100}) - ({}^{0.6}(n_a)_{60} - {}^{0.6}(n_a)_{100})\\
&\quad - ({}^{1.0}(n_c)_{60} - {}^{1.0}(n_c)_{100}) + ({}^{1.0}(n_a)_{60} - {}^{1.0}(n_a)_{100})],\\
a_3 &= {}^{0.6}(n_c)_{60} - {}^{0.6}(n_a)_{60} - {}^{1.0}(n_c)_{60} + {}^{1.0}(n_a)_{60} + 2/3[({}^{0.6}(n_a)_{60}\\
&\quad - {}^{0.6}(n_a)_{100}) - ({}^{0.6}(n_c)_{60} - ({}^{0.6}(n_c)_{100}) - ({}^{1.0}(n_a)_{60} - {}^{1.0}(n_a)_{100})\\
&\quad + ({}^{1.0}(n_c)_{60} - {}^{1.0}(n_c)_{100})],\\
b_0 &= a_0 + 2/5({}^{1.0}(n_b)_{60} - {}^{1.0}(n_c)_{60}) + 3/5[({}^{1.0}(n_b)_{60} - {}^{1.0}(n_b)_{100})\\
&\quad - ({}^{1.0}(n_c)_{60} - {}^{1.0}(n_c)_{100})],\\
b_1 &= a_1 + ({}^{1.0}(n_c)_{60} - {}^{1.0}(n_c)_{100}) - ({}^{1.0}(n_b)_{60} - {}^{1.0}(n_b)_{100})],\\
b_2 &= a_2 + ({}^{1.0}(n_a)_{60} - {}^{1.0}(n_a)_{100}) - ({}^{1.0}(n_c)_{60} - {}^{1.0}(n_c)_{100})].
\end{aligned}$$